UC San Diego
UC San Diego Previously Published Works

Title

Potent spinal parenchymal AAV9-mediated gene delivery by subpial injection in adult rats and pigs

Permalink

https://escholarship.org/uc/item/755704zm

Authors

Miyanohara, Atsushi
Kamizato, Kota
Juhas, Stefan
et al.

Publication Date

2016

DOI

10.1038/mtm.2016.46

Peer reviewed

npg

ARTICLE

Potent spinal parenchymal AAV9-mediated gene delivery by subpial injection in adult rats and pigs

Atsushi Miyanohara[1], Kota Kamizato[1], Stefan Juhas[2], Jana Juhasova[2], Michael Navarro[1], Silvia Marsala[1], Nada Lukacova[3], Marian Hruska-Plochan[4], Erik Curtis[5], Brandon Gabel[5], Joseph Ciacci[5], Eric T Ahrens[6], Brian K Kaspar[7], Don Cleveland[8,9] and Martin Marsala[1,3]

Effective *in vivo* use of adeno-associated virus (AAV)-based vectors to achieve gene-specific silencing or upregulation in the central nervous system has been limited by the inability to provide more than limited deep parenchymal expression in adult animals using delivery routes with the most clinical relevance (intravenous or intrathecal). Here, we demonstrate that the spinal pia membrane represents the primary barrier limiting effective AAV9 penetration into the spinal parenchyma after intrathecal AAV9 delivery. We develop a novel subpial AAV9 delivery technique and AAV9-dextran formulation. We use these in adult rats and pigs to show (i) potent spinal parenchymal transgene expression in white and gray matter including neurons, glial and endothelial cells after single bolus subpial AAV9 delivery; (ii) delivery to almost all apparent descending motor axons throughout the length of the spinal cord after cervical or thoracic subpial AAV9 injection; (iii) potent retrograde transgene expression in brain motor centers (motor cortex and brain stem); and (iv) the relative safety of this approach by defining normal neurological function for up to 6 months after AAV9 delivery. Thus, subpial delivery of AAV9 enables gene-based therapies with a wide range of potential experimental and clinical utilizations in adult animals and human patients.

Molecular Therapy — Methods & Clinical Development (2016) **3**, 16046; doi:10.1038/mtm.2016.46; published online 13 July 2016

INTRODUCTION

Over the past decade, several experimental and clinical studies reported on the successful use of adeno-associated virus (AAV)-based vectors (particularly AAV9) for central nervous system (CNS)-targeted gene delivery. These studies established unequivocally the value of AAV-based-delivery vectors as a tool to achieve a potent gene silencing or upregulation in targeted CNS regions and provided evidence that this therapeutic approach can effectively be used in treatment of numerous neurological disorders, including ALS, SMA, muscle spasticity, and chronic pain. Despite these encouraging data and extensive preclinical animal studies, detailed mechanisms on how the AAV vectors penetrate into the brain or spinal cord parenchyma after using different routes of AAV delivery (*e.g.*, systemic, intrathecal) are not fully understood. These data are critical for the development of new and more effective AAV delivery protocols that would be equally potent in young and in fully developed adult animals and in human patients. In general, preclinical animal studies can be categorized into several groups based on the developmental stage when the animal is employed or the route by which the AAV is delivered (systemic or intrathecal). Depending on the parameters used in the individual studies, the level of transgene expression and the specific cell populations (neuronal and/or glial) that are being infected vary greatly.

First, early studies have demonstrated that systemic-vein (i.v.) injection of AAV9-GFP in neonatal mice leads to widespread CNS green fluorescent protein (GFP) expression, including dorsal root ganglia, spinal motoneurons (MN), and neurons in the brain (neo-cortex, hippocampus, cerebellum). Using adult mice, i.v.-delivered AAV9-GFP leads to a preferential astrocyte infection throughout the entire CNS, but only limited neuronal expression is seen.[1] Comparable data were reported by Barkats *et al*.[2] who demonstrated widespread spinal MN GFP expression after systemic i.v. delivery of AAV9 in neonatal mice. In addition, the same group demonstrated successful transgene expression in spinal MN once AAV9 was delivered i.v. in adult mice or cats.[2] Similar to these two studies, Gray *et al*. have shown CNS neuronal GFP expression after i.v. AAV9 administration in adult mice, however, only limited transduction efficiency was seen in juvenile non-human primates; compared to a previous study performed by Foust and Kaspar *et al*.,[1] a clear shift from neuronal to glial expression was seen in the brain.[3]

Second, given the apparent limited neuronal expression after systemic i.v. AAV9 delivery in adult animals, use of the intrathecal route (to bypass the blood-brain barrier) was explored in several studies. Using 1-year-old, 2 kg BW, non-human primates (Cynomolgus macaques), it was demonstrated that a single lumbar-intrathecal injection of AAV9-CB-GFP led to 50–75% MN transduction in the

[1]Neuroregeneration Laboratory, Department of Anesthesiology, University of California, San Diego, California, USA; [2]Institute of Animal Physiology and Genetics, Czech Academy of Sciences, Libechov, Czech Republic; [3]Institute of Neurobiology, Slovak Academy of Sciences, Kosice, Slovak Republic; [4]Institute of Molecular Life Sciences, University of Zurich, Zurich, Switzerland; [5]Department of Neurosurgery, University of California, San Diego, California, USA; [6]Department of Radiology, University of California, San Diego, California, USA; [7]Department of Pediatrics, The Ohio State University, The Research Institute at Nationwide Children's Hospital, Columbus, Ohio, USA; [8]Ludwig Institute and Department of Cellular and Molecular Medicine, University of California, San Diego, California, USA; [9]Ludwig Institute and Department of Neurosciences, University of California, San Diego, California, USA. Correspondence: M Marsala (mmarsala@ucsd.edu)
Received 6 April 2016; accepted 14 May 2016

entire spinal cord at 2 weeks after AAV9 injection.[4,5] Similarly, in another study using juvenile 2- to 3-year-old nonhuman primates (Cynomolgus macaques) or young (2-month-old) pigs, potent MN transduction was seen throughout the entire spinal cord after intra-cisternal or combined cisternal-lumbar intrathecal AAV9 delivery. In addition, in the same study, GFP expression was observed in dorsal root ganglion cells, motor cortex and in Purkinje cells in the cerebellar cortex.[6] In a more recent study, comparable lumbar MN GFP expression was seen in nonhuman primates (Cynomolgus macaques) after intra-cisternal AAV9-GFP injection.[7]

Interestingly, in all studies that employ a cisternal or lumbo-sacral intrathecal delivery route, the available histological data show a very specific spinal transgene expression pattern. It is characterized by intense expression in α-motoneurons. However, the ventral horn interneurons, which reside in close proximity to the GFP-expressing α-motoneurons, appear to be transgene negative. Similarly, potent transgene expression is seen in dorsal root ganglion cells and primary afferents. However, small interneurons localized in the superficial dorsal horn or in the intermediate zone show no transgene expression.

This high level of transgene expression selectivity and lack of transduction in deeper gray matter cells indicates the presence of a well-developed regulatory-barrier system (in addition to blood–brain barrier) that prevents the penetration of virus into deeper spinal compartments from the intrathecal space. Based on the well-described anatomical organization of spinal meninges, we hypothesized that the pia mater represents the key barrier that regulates the penetration of AAV into the spinal parenchyma after intrathecal AAV delivery. We also speculate that the high level of transgene expression seen in MN and DRG cells reported after IT delivery is likely mediated by the preferential retro- and antero-grade infection of axons projecting into and out of the spinal parenchyma and trans-passing the IT space (*i.e.*, ventral and dorsal roots).

Accordingly, to address this issue, we have developed and validated a subpial (SP) vector delivery method in adult rats and pigs and provide evidence that this delivery route leads to potent trans-spinal transgene expression infecting the entire population of neurons in the gray matter of subpially-injected segments. In addition, near complete infection of descending and ascending axons was achieved and corresponded with the transgene expression in brain centers (motor cortex, nucleus ruber). Overall, this study provides one of the first evaluations of the mechanism by which AAV9 vectors target cells throughout the CNS.

RESULTS

Effective spinal parenchymal AAV9-mediated transgene expression after single bolus subpial AAV9-UBI-GFP (or -RFP) injection in adult rats and pigs

We first tested the potency of single bolus subpial AAV9-UBI-GFP or AAV9-UBI-RFP delivery in rats and pigs (Figures 1 and 2; Supplementary Figure S1). Animals received 30 µl (rats) or 200 µl (pigs) of AAV9 vector in 2.5% dextran solution delivered into the subpial space of cervical (C4-6), thoracic (Th6-9) or lumbar (L2-L5) segments. At 8 weeks after AAV9 delivery, spinal cords were dissected from 4% paraformaldehyde perfusion-fixed animals and imaged in situ using an Avis fluorescence system. Transverse or horizontal spinal cord sections were then cut from AAV9-injected segments and analyzed for the presence of GFP or red fluorescent protein (RFP) and costained with neuronal (NeuN), glial (glial fibrillary acidic protein (GFAP), CC1) and endothelial (RECA-1) antibodies. No anti-GFP or anti-RFP antibodies were used in any of the staining combinations presented and the captured GFP and RFP signals represent a "true"

transgene expression. In both rat and pig spinal cords, an intense GFP or RFP expression was seen on the surface of the spinal cord and was readily identified by visual inspection as yellow-green or red areas. Figure 1h,j shows the presence of RFP (red color) in transversely cut pig spinal cord and in the ventral roots (H-insert) in comparison to naive spinal cord (**i**). Correspondingly, the spinal surface densitometric analysis of AAV9-UBI-GFP-injected animals (rats and pigs) showed a widespread GFP signal extending for up to 5–10 cm from the epicenter of the subpial AAV9 delivery (Figure 1f,g).

Using horizontally cut spinal thoracic sections taken from pigs previously injected SP with AAV9-UBI-RFP in the mid-thoracic level (the same spinal cord as shown in Figure 1h), extensive parenchymal RFP expression was seen. The RFP expression was readily identified in the majority of interneurons and α-motoneurons and extended throughout four to six spinal segments (Figure 2a,b). Similarly, intense RFP expression in the axo-dendritic arbor was seen throughout the whole RFP-expressing gray matter (Figure 2a,b—white asterisks).

Analysis of transverse spinal cord sections taken from the epicenter of SP AAV9 injection confirmed intense RFP expression throughout the white and gray matter. In the white matter, a punctate-like RFP expression was seen in the majority of transversally-cut axons (Figure 2c—white asterisks—yellow box inserts) and were identified in dorsal, lateral and ventral funiculi (Figure 2c—DF, LF, VF; yellow box inserts). In the gray matter, numerous interneurons distributed between laminae I-IX and ventral α-motoneurons showed intense RFP expression in soma and in axo-dendritic arbor. A high density of RFP expression was also seen in the terminal boutons throughout the gray matter (Figure 2d–g). Similarly, confocal analysis showed the presence of RFP signal in astrocytes (Figure 2c—insert: RFP/GFAP). In transverse spinal cord sections taken from naive pigs stained with NeuN antibody and developed with FITC secondary antibody, no background RFP signal was detected once images were captured with both 488 and 594 filters (Figure 2h).

A similar neuronal GFP expression pattern was seen in the rat lumbar spinal cord after SP AAV9-UBI-GFP injection at the L1-2 level. A high density of GFP+ neurons throughout the L1-L5 lumbar segments localized in the whole gray matter between laminae I-IX were identified (Supplementary Figure S1a).

A quantitative segmental analysis of GFP expressing neurons (α-motoneurons and interneurons) in rats (*n* = 3) and pigs (*n* = 3) receiving upper lumbar (L1-2) subpial AAV9-UBI-GFP injection and surviving for 6 months is shown in Table 2. In general, a consistent high-level neuronal transgene expression was seen in five to seven segments above and below the site of AAV9 injection. No neuronal transgene expression was seen in cervical neurons after lumbar subpial AAV9 delivery or in lumbar neurons after cervical subpial AAV9 delivery.

Descending motor axon GFP expression in spinal segments distant from the site of subpial AAV9-UBI-GFP delivery

We next characterized the extent of descending spinal tract GFP expression in the lumbar spinal cord after SP injection of AAV9-UBI-GFP into the subpial space of the mid-thoracic (Th6-7) or lower cervical segments in both rats and pigs. At 3–6 weeks after SP AAV9 delivery, intense GFP expression was seen throughout the whole lumbar spinal cord. Using transverse lumbar (L2-L6) spinal cord sections taken from pigs, high-intensity GFP expression in transversely-cut axons in the lateral and ventral funiculi was readily identified without additional GFP immunostaining (Figure 3a; white asterisks). In these regions, a similar density of GFP+ axons was seen throughout the whole white matter. In comparison to lateral and ventral funiculi, a
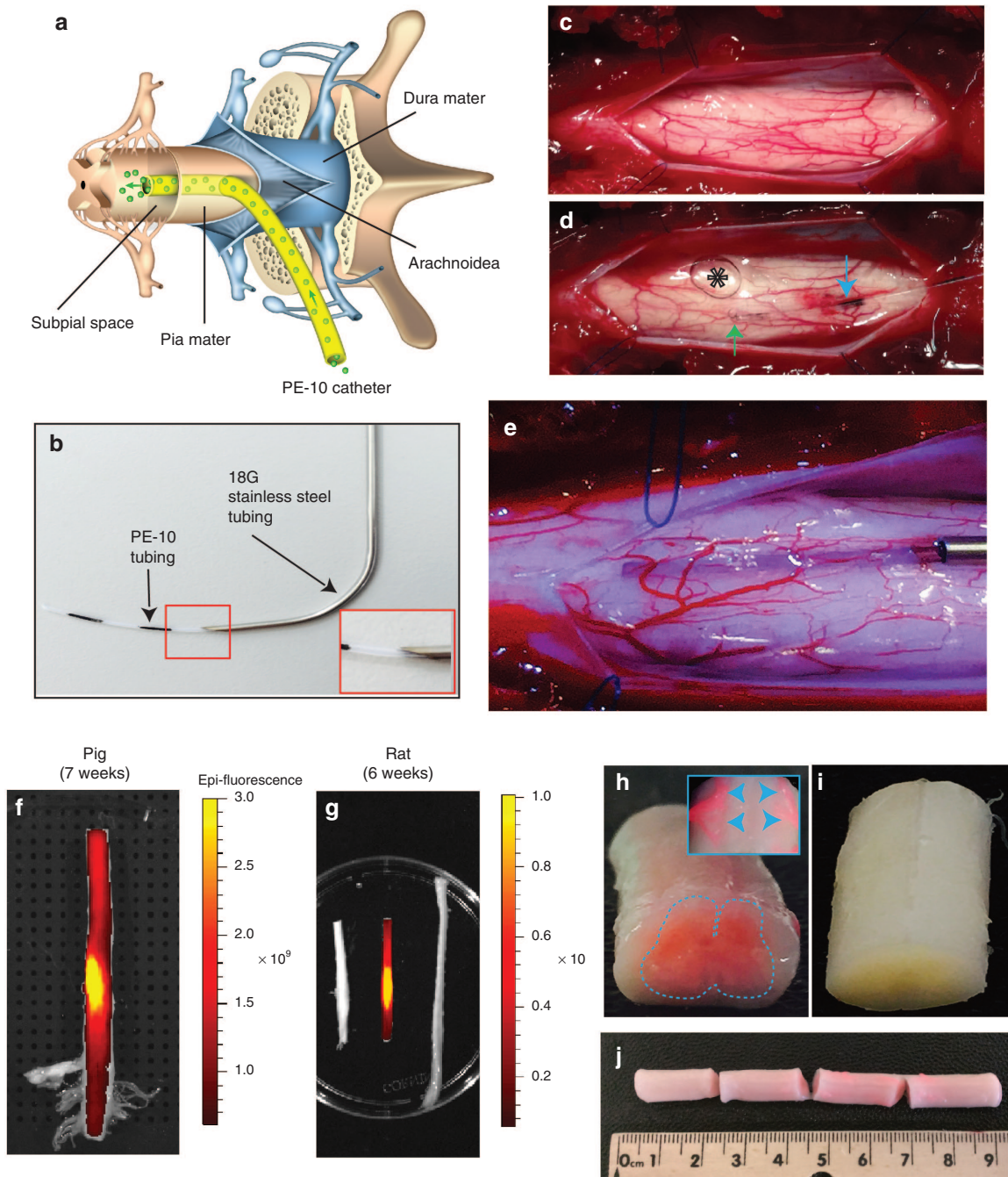
Figure 1 Technique of subpial AAV9 delivery and macroscopically defined spinal cord surface transgene expression. (**a**) Schematic drawing of spinal cord, meninges and sub-pially placed PE-10 catheter in pigs. (**b**) A catheter guiding tube (18G) is used to advance the PE-10 catheter into the subpial space. (**c–e**) To place the catheter into the subpial space, the dura mater is first cut open (**c**) and the catheter is advanced into the SP space (**d,e**). An air bubble injected into the subpial space can be seen (**d**-asterisk). (**f,g**) Surface GFP fluorescence densitometry shows an intense signal in both rat and pig spinal cord with the most intense GFP fluorescence seen at the epicenter of lumbar subpial injection. (**h–j**) The presence of intense RFP fluorescence in the spinal cord parenchyma detected macroscopically in pig thoracic spinal cord (**h,j**). A clear high level of RFP expression in ventral roots can also be seen (**h**-insert). No fluorescence in the control noninjected spinal cord can be identified (**i**).

relatively lower number of GFP+ axons was seen in the dorsal funiculi (Figure 3a; DF). Consistent with the degree of axonal labeling seen in the white matter of lateral and ventral funiculi, a dense network of GFP+ axons terminating in the gray matter was seen (Figure 3a,b). These axons were identified between laminae III-X. Only a few GFP+ axons in the lamina I-III were seen. High-power confocal microscopy showed a high density of fine GFP+ axons with numerous terminal boutons in the gray matter (Figure 3c).

A comparable GFP expression pattern in descending motor axons in the lumbar gray matter was seen in rats previously receiving upper cervical SP injection of AAV9-UBI-GFP (Supplementary Figure S1b).

Effective retrograde transgene expression in brain motor regions after spinal subpial AAV9-UBI-GFP delivery in rats and pigs
Analysis of transgene (GFP) expression in brain motor centers (motor cortex, nucleus ruber, and formatio reticularis) at 6 weeks after SP
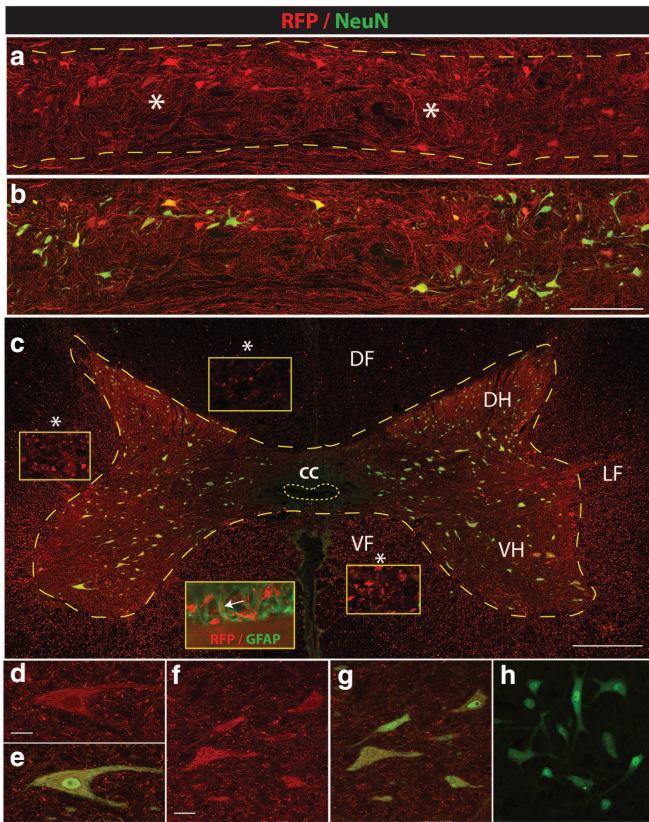
Figure 2 Effective parenchymal AAV9-mediated transgene expression after single bolus subpial AAV9-UBI-RFP injection in adult pigs. (**a,b**) Horizontal spinal cord sections taken from the mid-thoracic spinal cord of pigs injected with AAV9-UBI-RGF 6 weeks previously. Intense RFP expression can be seen throughout the whole region, including the white and gray matter. Staining with NeuN antibody (green) shows that virtually all neurons are also RFP positive. (**c–g**) Transverse spinal cord section taken from the SP-injected region shows transversally-cut RFP+ axons in the dorsal (DF) lateral (LF) and ventral (VF) funiculus (yellow box inserts). RFP expression can also be seen in glial fibrillary acidic protein (GFAP)-stained astrocytes (**c** insert; RFP/GFAP). High density RFP+ terminal boutons surrounding RFP-expressing α-motoneuron (**d,e**) and interneurons (**f,g**) can be seen. (**h**) Transverse spinal cord section taken from the mid-thoracic spinal cord in a naive animal and stained with anti-NeuN antibody. Image was acquired using 488 and 594 filter and the identical settings as used in Figure 2f. No detectable background RFP signal can be seen (**Sca**le bars: **a–c**-500 µm; **d, f**-30 µm).

AAV9-UBI-GFP delivery (*n* = 2) in pigs showed intense GFP-labeled pyramidal neurons in the motor cortex (Figure 4a–e). Similarly, numerous GFP+ neurons localized in the brain stem were identified (Figure 4f–j). Consistent with the presence of GFP+ neurons in the motor cortex, a high number of GFP+ corticospinal axons in the ventral region of the medulla oblongata (medullary pyramids) was seen (Figure 4k). In addition, a high density of anterogradely labeled GFP+ spinoreticular terminals was seen throughout the reticular formation (Figure 4l), as well as in spinothalamic terminals in the thalamic nuclei (not shown).

Comparably as seen in pigs, using sagittal sections taken from the medulla oblongata and cerebellum in rats, a high density of GFP+ fiber network was identified at 8 weeks after cervical subpial AAV9-UBI-GFP injection (Figure 5a–c). In addition, clearly labeled spinocerebellar tract fibers in the cerebellum were seen (Figure 5a; insert).

Using coronal sections taken from the brain stem and motor cortex, intense labeling of nucleus ruber neurons (NR), ascending spinothalamic fibers in the medial lemniscus (ML) and descending
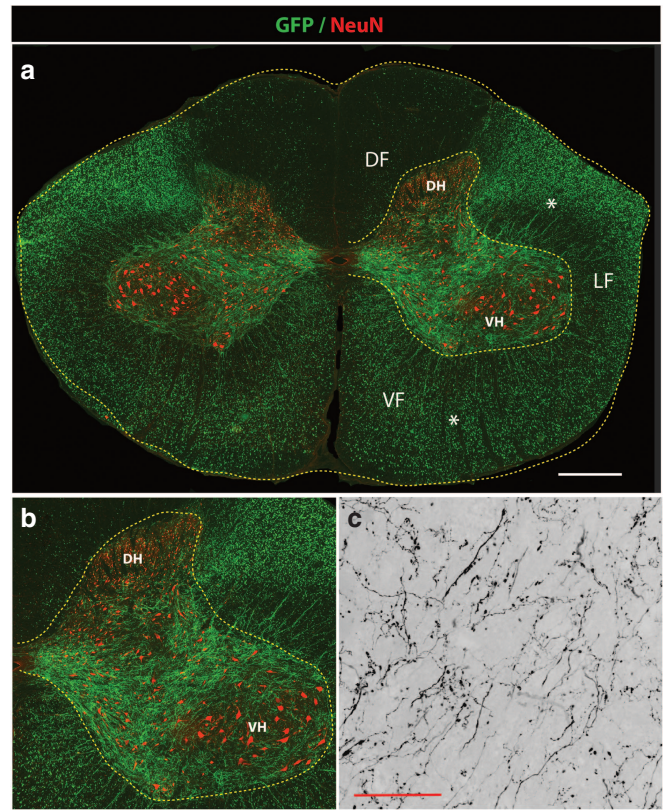
Figure 3 Potent GFP expression in descending motor axons in lumbar spinal cord after mid-thoracic subpial AAV9 injection in adult pigs. (**a,b**) Transverse spinal cord section taken from the lumbar spinal cord after subpial AAV9-UBI-GFP injection into the mid-thoracic subpial space 6 weeks prior. Intense GFP expression in transversal cut axons in lateral (LF) and ventral (VF) funiculus can be seen (white asterisks). A relatively lower density of GFP+ axons in the dorsal funiculus was identified (DF). Correspondingly, a high density of GFP+ motor axons projecting into the gray matter localized between the dorsal horn (DH) and ventral horn (VH) can also be seen. (**c**) A higher resolution confocal image shows very fine arborization of GFP+ axons and terminal boutons in the central gray matter (Scale bars: **a**-1,000 µm; **c**- 30 µm). DF, dorsal funiculus; DH, dorsal horn; LF-lateral funiculus; VF, ventral funiculus; VH, ventral horn.

corticospinal tract (CPD; cerebral peduncle) was consistently seen (Figure 6a). Corresponding to the intense corticospinal tract labeling seen at the level of the brain stem and medulla oblongata, clear GFP expression in cortical neurons in layer V was seen. No GFP expression in other cortical layers was identified (Figure 6b; insert No. 3).

Differential regional spinal transgene expression after intrathecal versus subpial AAV9 delivery

We next compared the distribution of spinal transgene expression after the AAV9-UBI-GFP was injected into the lumbar intrathecal (*N* = 5) or lumbar subpial (L1-L2; *N* = 4) space (Figure 7a–f). After AAV9 delivery, animals survived for 3 months.

IT injection of AAV9-UBI-GFP led to intense GFP expression in the dorsal funiculus, primary afferents in the dorsal horn (lamina II-III) and in the medial part of lamina V-VII. Several GFP+ Ia afferents terminating in the ventral horn in the vicinity of large α-motoneurons were also identified (Figure 7a; lower right insert). Consistent with high GFP expression in primary afferents, a high number of GFP+ neurons were found in the dorsal root ganglion cells (Figure 7a; upper right B/W insert). The clear presence of increased GFP expression was also consistently seen
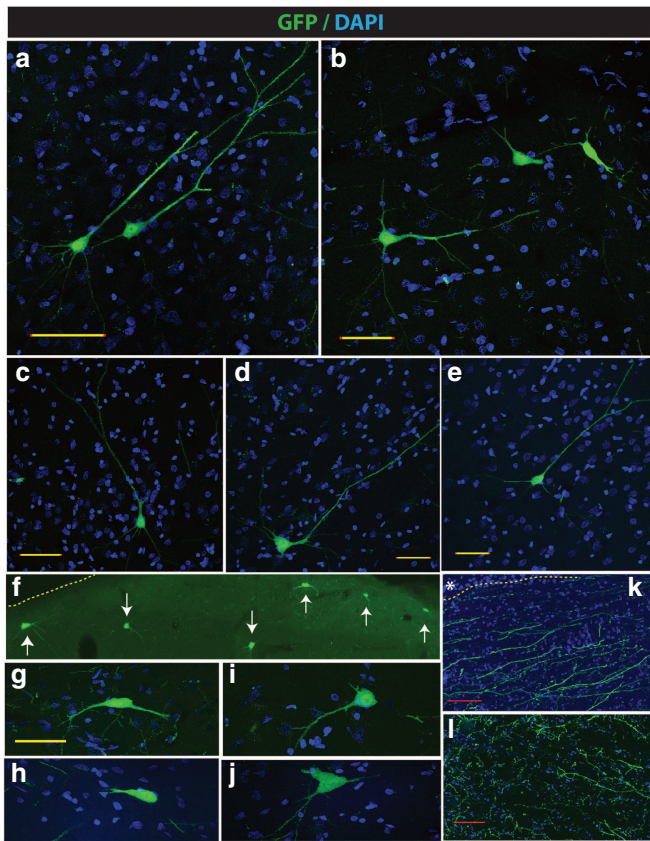
GFP / DAPI

Figure 4 Retrograde infection-mediated GFP expression in brain motor centers after subpial mid-thoracic AAV9 delivery in adult pigs. (**a–e**) Retrogradely labeled pyramidal neurons in the motor cortex of pigs at 6 weeks after a mid-thoracic single AAV9-UBI-GFP injection. (**f–j**) A comparable level of GFP expression in neurons localized in the brain stem can be seen. (**k**) Presence of large retrogradely-labeled motor GFP+ axons in the medulla oblongata (medullary pyramids) can be identified. (**l**) A high density of anterogradely labeled sensory afferents in formatio reticularis (Scale bars: **a–e** and **g–j**-50 μm; **k, l**-50 μm).

Calbindin / GFP

Figure 5 Retrograde and anterograde-transport-mediated GFP expression in medulla oblongata and cerebellum at 8 weeks after subpial cervical AAV9 delivery in adult rats. (**a–c**) An intense GFP expression in medulla oblongata representing a mixture of retrogradely and anterogradely labeled axons can be seen. A fine arborization of GFP-expressing spino-cerebellar tract terminals in the cerebellum can also be identified (**a**; insert) (Scale bar: **a**-2 mm; insert-200 μm; **b, c**-500 μm).

around the ventral root entry zone (Figure 7a; left bottom insert). Several GFP expressing glial cells were seen in this region. In the ventral gray matter, some α-motoneurons showed GFP expression (Figure 7a; lower right insert). Except for these regions, and cell groups that showed GFP expression, almost a complete lack of neuronal or glial GFP expression was seen in other deeper regions of the gray matter, including the dorsal horn, intermediate zone and in the white matter of the lateral and ventral funiculi (Figure 7a–c). Interestingly, even the neurons localized in the superficial dorsal horn and which reside in close vicinity to the intrathecal space (but separated by pia mater) showed a complete lack of GFP expression (Figure 7c).

In contrast to the GFP expression pattern seen after intrathecal AAV9-UBI-GFP delivery, the GFP expression resulting from lumbar subpial AAV9 injection showed a substantially different regional expression pattern and was similar to that seen in adult pigs. Intense GFP expression was seen in the majority of interneurons and α-motoneurons in the SP-injected segment (Figure 7d–f) as well as in segments localized rostral and caudal from the site of SP AAV9 injection (Supplementary Figure S1a; Table 2). Corresponding with high α-motoneuronal GFP expression, a consistent GFP signal was seen in ventral root axons (Figure 7d; VR). Likewise, a high intensity of GFP expression was seen in virtually
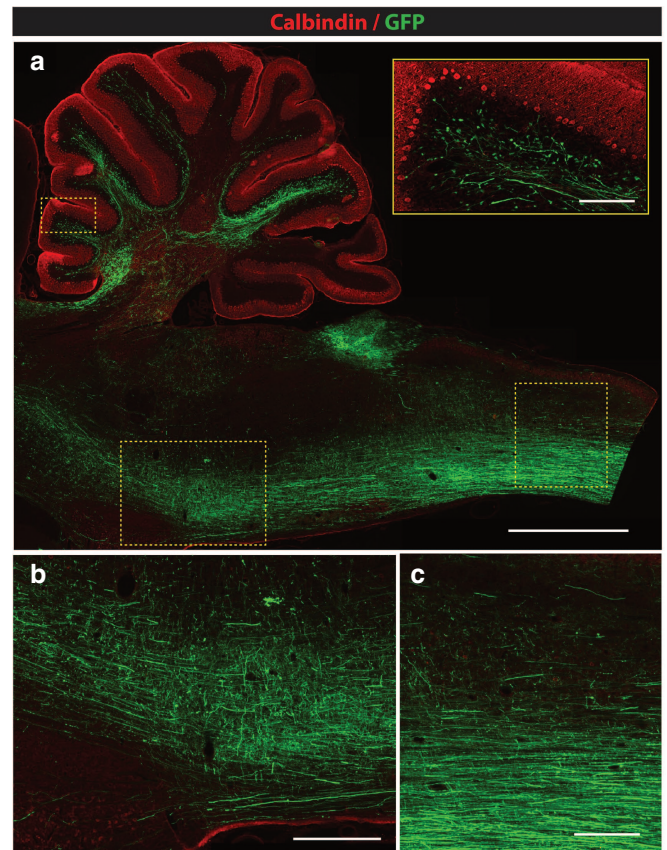
all axons in the lateral and ventral funiculi (Figure 7d; LF, VF). Similarly as seen in pigs, rats that previously received cervical SP AAV9 injection, a high density of GFP+ axonal network was seen in segments distal to the site of cervical injection in all thoraco-lumbo-sacral segments (Supplementary Figure S1b).

Expression of GFP in glial and endothelial cells after lumbar subpial AAV9-UBI-GFP delivery in rats
We next tested the cellular specificity of GFP expression at 6 months after lumbar subpial injection of AAV9-UBI-GFP in rats. Staining with anti-GFAP, CC1 and RECA-1 antibodies and confocal analysis showed clearly detectable GFP expression in glial and endothelial cells (Figure 8a–i).

Long-term+ neurological effect of lumbar subpial AAV9-UBI-GFP delivery in rats and pigs
Periodic analysis of motor and sensory (allodynia) function in rats (*n* = 6) showed no detectable deficit for 6 months post-AAV9 delivery. A transient motor weakness (motor score: 10) was seen in one of four pigs between 3–21 days after AAV9-delivery. The same animal also showed increased vocalization to skin pinch (*i.e.*, allodynia). Allodynia and motor weakness were no longer present at intervals longer than 30 days after AAV9 injection.
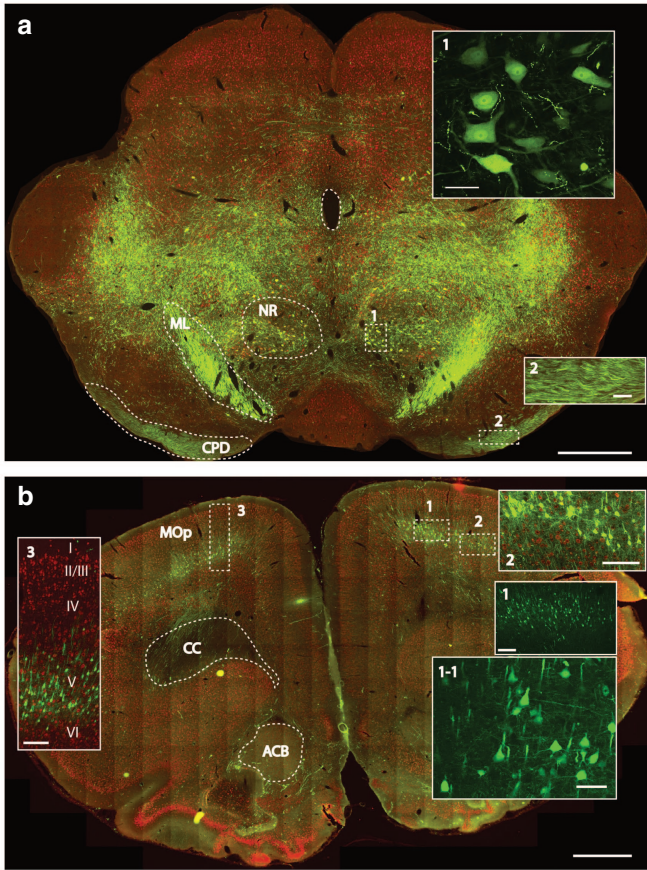
npg

Potent spinal parenchymal AAV9-mediated gene delivery by subpial injection in adult rats and pigs
A Miyanohara *et al*.

6

Figure 6 Retrograde and anterograde-transport-mediated GFP expression in the brain stem and motor cortex at 8 weeks after subpial cervical AAV9 delivery in adult rats. (**a**) Intense bilateral GFP expression can be seen throughout the brain stem (NR, nucleus ruber; ML, medial lemniscus; CPD, cerebral peduncle). (**b**) Specific and intense GFP expression in retrogradely-labeled pyramidal neurons in the motor cortex (layer V) can be identified (MOp-primary somatomotor area; CC-corpus callosum; ACB-nucleus accumbens) (Scale bars: **a**-1 mm; inserts No.1 and No.2–50 μm; **b**-1mm; inserts No.1–250 μm; No.1-1-50 μm; No.2 and No.3–250 μm).

DISCUSSION

Surgical-technical and safety considerations of subpial catheter placement

To place the SP catheter in adult rats or pigs, several sequential procedural steps are followed to minimize potential spinal injury associated with instruments/catheter manipulation in the vicinity of the exposed "dura-free" spinal cord. First, the use of caudal and cranial spinal clamps (placed just above and below the laminectomy) proved to be essential in minimizing spinal cord pulsation during catheter placement. Second, an "L" shaped catheter-guiding stainless steel tube mounted on an XYZ manipulator is used for SP catheter placement. The pia is first punctured using a bent 30G needle. Once the tip of the penetrating 30G needle is in the subpial space for about 1–1.5 mm, the pia is slightly lifted for 1–2 mm. A PE-10 catheter (pigs) is then placed into the SP space by advancing the catheter from the guiding tube. After the catheter is advanced to the targeted length, the penetrating needle is removed from the SP space. Once the vector injection is completed (typically over 3 minutes), the catheter is slowly pulled out of the SP space and the dura is closed. By using this technical approach, the placement of the SP catheter takes an average of 3–5 minutes from the moment of dura opening. Currently, we have placed the SP catheter in over 25 pigs
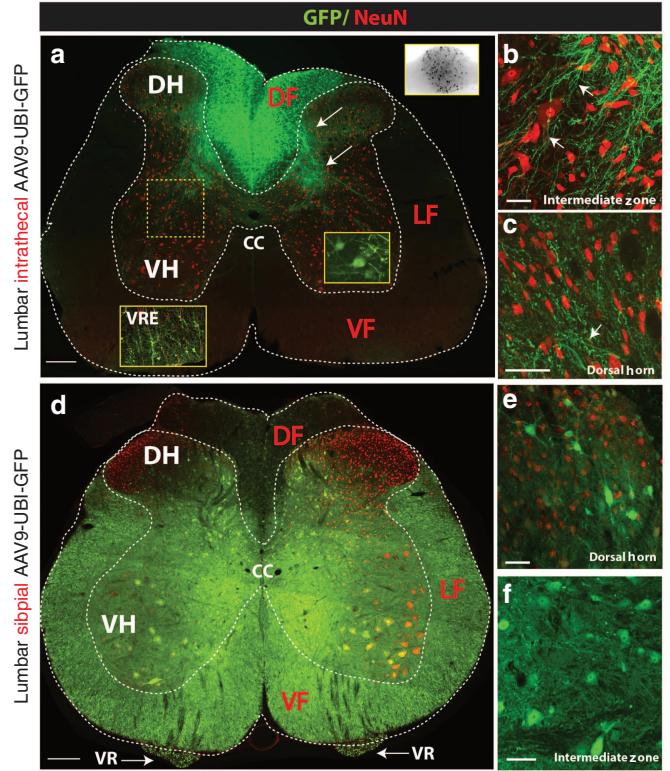

Figure 7 Differential regional spinal transgene expression after intrathecal AAV9-UBI-GFP versus subpial AAV9-UBI-RFP delivery in rats. (**a–c**) Lumbar intrathecal injection of AAV9-UBI-GFP led to the preferential GFP expression in the dorsal funiculus (DF), primary afferents distributed in the dorsal and ventral gray matter (white arrows) and dorsal root ganglion neurons (**a**; upper-right BW insert). A subpopulation of α-motoneurons and glial cells localized in the ventral root entry zone (VRE) also show GFP expression (yellow right insert; white left insert-VRE). No or minimal GFP expression in axons localized in the lateral (LF) or ventral funiculi (VF) was seen. Similarly, no GFP expression in interneurons in the dorsal horn or in the intermediate zone could be detected (**b, c**). (**d–f**) In contrast to intrathecal injection, the lumbar subpial injection of AAV9-UBI-GFP led to widespread transgene expression. Numerous GFP expressing NeuN+ neurons localized throughout the gray matter, including interneurons and α-motoneurons, were seen (**e, f**). Consistent with α-motoneuronal GFP expression, high GFP expression was seen bilaterally in transversely cut motor axons in the ventral roots (**d**; VR). Similarly, high intensity of GFP was seen virtually in all transversely cut axons in the lateral and ventral funiculi (Scale bars: **a**, D-200 μm; **b, c, e**-50 μm; **f**-20 μm). CC, central canal; DF, dorsal funiculus; DH, dorsal horn; LF, lateral funiculus; VF, ventral funiculus; VH, ventral horn; VR, ventral root; VRE, ventral root entry zone.

using this technique and achieved consistent and injury-free SP catheter placement. In our early attempts, we tried the SP catheter placement by free hand (without the use of a guiding tube and XYZ manipulator). These attempts were unsuccessful and resulted in local spinal cord injury and bleeding and/or inconsistent placement of the catheter in the SP space with some catheters penetrating the superficial layers of the spinal cord tissue. An identical technique is used in adult rats, however, a PE-5 catheter is used instead.

Subpial AAV9 delivery leads to widespread transgene expression in neurons throughout the gray matter and ascending and descending axons in SP-injected segments

As we have shown in our present study, a single subpial AAV9 injection led to potent parenchymal transgene expression spreading rostro-caudally for multiple segments. In adult pig spinal cord,
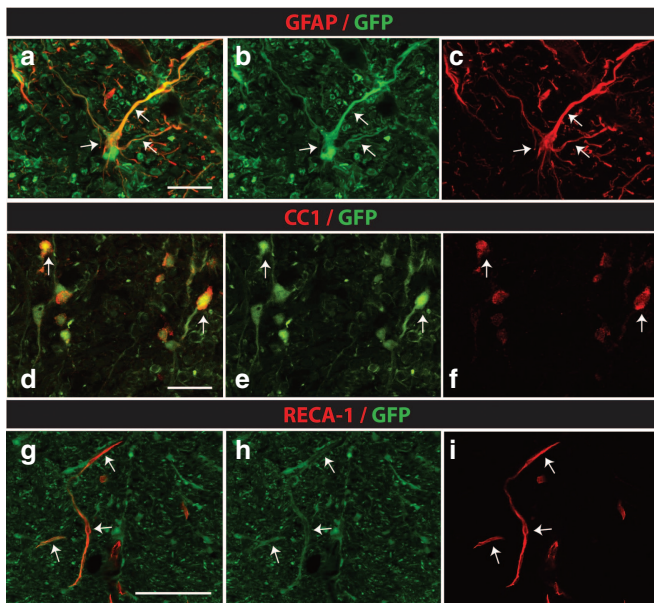
Potent spinal parenchymal AAV9-mediated gene delivery by subpial injection in adult rats and pigs
A Miyanohara et al.

npg

7

Figure 8 Expression of GFP in glial and endothelial cells in lumbar spinal cord at 6 months after subpial AAV9-UBI-RFP delivery in rats. (**a–i**) Confocal analysis of GFP-expressing cells in the lumbar spinal cord at 6 months after subpial AAV9-UBI-GFP delivery in rats shows consistently labeled astrocytes (**a–c**; white arrows), oligodendrocytes (**d–f**; white arrows) and endothelial cells (**g–i**; white arrows) (Scale bars: **a, d, g**-30 μm).

the transgene spread was consistently seen at distances ranging between 10–15 cm. Expression was identified in neurons and glial cells in all gray matter laminae and in axons in ventral, lateral and dorsal funiculi, confirming a near complete penetration of SP-injected AAV9 vector throughout the spinal parenchyma. By analyzing transverse lumbar spinal cord sections in pigs that received a mid-thoracic AAV9-UBI-GFP injection (i.e., about 30 cm distance from the site of AAV9 delivery), virtually all descending motor axons appear to be labeled at 6 weeks after AAV9 injection. Higher-resolution confocal microscopy revealed a dense network of fine axonal arborizations with terminal boutons throughout the gray matter. Consistent with the level and distribution of infected axons in the white matter, retrogradely infected GFP-expressing neurons in the motor cortex and brain stem were identified. Similarly, centrally projecting sensory axons were identified in the reticular formation and in the thalamus. In comparison to rats, the number of retrogradely infected cortical or brain stem neurons was relatively lower in pigs. Because the analysis of brain GFP expression in pigs was done in animals receiving mid-thoracic SP AAV9 injection (and not cervical SP AAV9 injection as done in the rats), a relatively lower number of labeled cortical/brain stem motor neurons may reflect a lower number of descending motor axons that were retrogradely infected at the mid thoracic spinal cord.

Pia mater represents a primary barrier for effective parenchymal penetration of AAV9 after intrathecal delivery
By comparing the transgene expression pattern after SP versus IT AAV9 delivery in rats, we have demonstrated a substantially different regional-cellular expression. First, after intrathecal delivery, the expression was only seen in regions and neuronal-glial pools that are morphologically associated with the dorsal and ventral root entry zone. Thus, potent transgene expression was seen in primary afferents and was clearly present in the dorsal funiculi,

primary afferents in the dorsal horn and Ia afferents projecting to the ventral horn. This transgene expression in primary afferents corresponded with potent expression in dorsal root ganglion cells. Similarly, clear expression was seen around the ventral root entry zone with some retrogradely labeled α-motoneurons in the ventral horn. In contrast, however, the transgene expression was virtually absent in all other neurons between laminae I-VII and X. Moreover, no descending motor axons were labeled in the lateral or ventral funiculi. These data jointly suggest that the spinal parenchymal GFP expression (whether in neurons or projecting primary afferents) is almost exclusively caused by retrograde or anterograde transgene expression and not by AAV9 uptake into the spinal parenchyma from the intrathecal space. This observation is consistent with data from other laboratories that demonstrate potent α-motoneuron GFP expression after a single intrathecal or cisternal AAV9-GFP injection in adult nonhuman primates or juvenile pigs. However, no interneuronal GFP expression is seen in interneurons residing in close proximity to GFP+ α-motoneurons.[4–7]

In contrast, as described above, the subpial AAV9 delivery was associated with potent transgene expression in the gray matter neurons (α-motoneurons and interneurons) and virtually in all descending motor axons and primary afferents of injected segments. These data clearly demonstrate that the pia mater represents the primary barrier preventing the penetration of AAV9 into other spinal cord compartments which are distant from the ventral and dorsal root entry zone. By bypassing the pial membrane and depositing the AAV9 into the subpial space, a trans-parenchymal infection of white and gray matter can be effectively achieved in adult rodents or large animals.

Potential clinical and experimental utilization of subpial AAV9 delivery
The potency of SP-induced infection and the neuronal cell populations that are being infected in the spinal cord and brain in adult animals have several potential clinical and experimental implications. First, in cases when a specific gene is to be silenced/downregulated (such as mutant SOD1 gene in ALS), a single cervical subpial injection of the silencing AAV9 construct will lead to effective gene silencing in cervical neurons and glial cells, in descending motor axons throughout the whole length of spinal cord and in the majority of ascending sensory fibers. Given well-characterized neurodegenerative patterns in amyotrophic lateral sclerosis(ALS) patients and experimental models of ALS that display progressive degeneration of upper motor neurons, projecting descending motor axons and lower motor neurons,[8–10] the ability to achieve widespread mutant gene silencing will likely provide a substantial advantage in achieving the most potent therapeutic effect. In addition, a single cervical SP injection can be combined with an additional SP injection into the lumbar enlargement to target the lumbar neuronal/glial population or with lumbar intrathecal injection to target α-motoneuronal pools throughout the thoracic and lumbar spinal cord. Second, increased expression of therapeutic genes (e.g., growth factors) associated with axonal sprouting can be readily achieved in descending motor tracts as well as ascending sensory fibers. For example, this could be tested for treatment potency in spinal trauma studies. In the case of the AAV9 vector, it can be administered from a single laminectomy site at the injury epicenter; the SP catheter could be advanced rostrally and caudally to target the distal end of severed motor axons and proximal ends of ascending sensory axons, respectively. Third, near complete descending motor tract labeling, which can be achieved from cervical SP AAV9-GFP injection, will enable studies of axonal sprouting and

synapse formation between labeled motor axons of the host and spinally grafted cells. Such data systematically characterizing the level of axonal sprouting and/or the development of synaptic contacts in cell-grafted large animal models of spinal injury are currently not available.

Pros and cons of using subpial gene delivery technique

As described, the primary advantage of SP AAV9 delivery, if compared to intrathecal delivery, appears to be superior spinal transparenchymal transgene expression. In addition, a comparable high-level of transgene expression is achieved in both adult rats and minipigs. Because the dimension of the spinal cord in adult 35–40 kg pigs is similar to humans, it is expected that a similar parenchymal AAV9 uptake will also be achieved in adult humans.

One of the limitations of the SP delivery technique is the requirement to perform local laminectomy to gain access to the dorsal surface of the SP-injected spinal cord. The requirement for laminectomy can limit its repetitive use, compared to intrathecal delivery, which can be used repetitively. However, the degree of transgene expression that can be achieved after SP AAV9 delivery appears to balance, if not surpass, this limitation should a clear and more potent therapeutic effect be seen once SP-based gene delivery is used in disease modifying studies. In addition, we have recently observed a sustained high-level of spinal GFP expression at 12 months in the lumbar spinal cord in naive-control rats and pigs receiving AAV9-UBI-GFP (unpublished observation). This would indicate that a single SP delivery of a therapeutic gene could potentially lead to a long-lasting effect before additional gene delivery needs to be considered.

Recent studies using nonhuman primates have demonstrated a substantial pathology and inflammatory changes in the cerebellum after intracisternal delivery of AAV9-encoding GFP (a non-self protein derived from jellyfish). Importantly, in the same study it was demonstrated that the expression of human aromatic L-amino acid decarboxylase (hAADC), a self-protein, has minimal proinflammatory and neurodegenerative effects.[11] While the degree of inflammatory changes caused by GFP or RFP expression was not specifically addressed in our current study, the behavioral data show normal neurological (motor and sensory) function in rats and pigs at chronic stages (up to 6 months) after subpial AAV9-UBI-GFP delivery. These data would suggest that even if inflammatory changes were present, these do not have a major neurological function-deterioration effect. Nonetheless, as demonstrated in previous nonhuman primate study,[11] careful consideration needs to be paid into the design of control-reporter or combined reporter-treatment AAV9 vectors to be used in the preclinical safety as well as efficacy studies.

Conclusion

Using adult rats and pigs, we have developed a novel subpial spinal cord AAV9 delivery technique that permits widespread transgene expression in the spinal parenchyma, descending and ascending axons, and does not require direct spinal cord tissue needle penetration (see summary diagram, Figure 9). In addition to spinal regional transgene expression, robust retrograde expression in brain motor centers was seen. This technique can potentially be used in preclinical studies and human clinical trials designed to upregulate or downregulate a gene of interest in specific spinal cord segments and/or in projecting motor and ascending sensory axons. The simplicity of this approach and potency of transgene expression in adult animals suggest that this technique may be successfully used in the adult patient
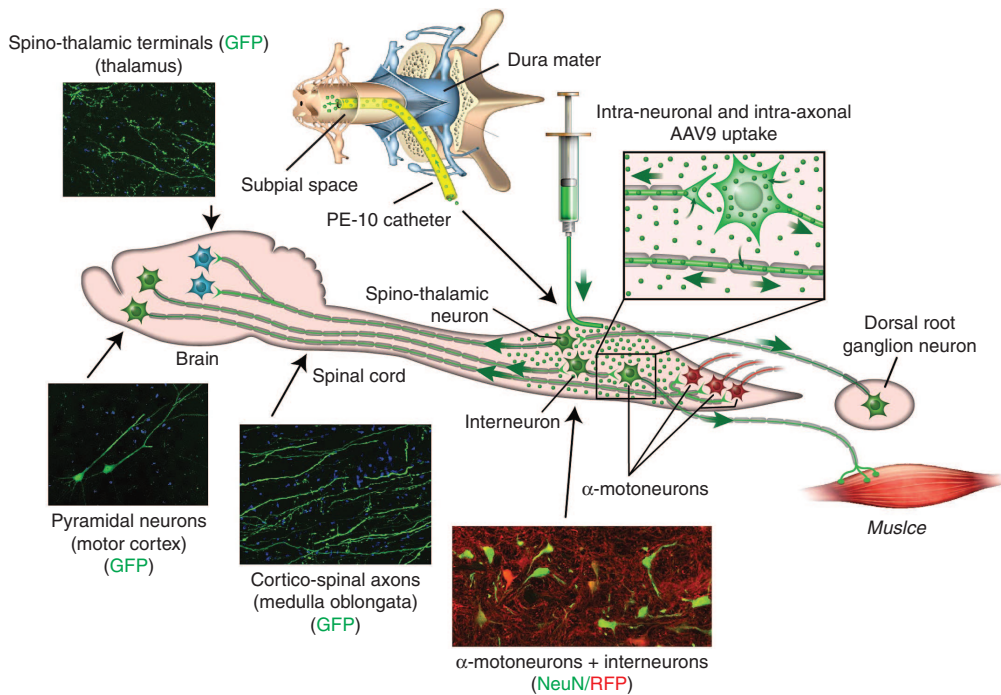

Figure 9 Schematic diagram demonstrating the technique of subpial AAV9 delivery and resulting transgene (GFP) expression throughout the CNS after a single subpial AAV9-UBI-GFP injection. The AAV9-UBI-GFP virus is delivered into the subpial space using a PE-10 catheter in adult pigs. Subpial delivery of AAV9-UBI-GFP leads to diffusion and resulting uptake of virus into segmental neurons (interneurons and α-motoneurons) and ascending and descending axons that are trans-passing through the SP-injected segments. Resulting transgene expression is then seen in: (i) segmental neurons, (ii) dorsal root ganglion cells (retrograde infection), (iii) motor axons innervating skeletal muscles (anterograde infection), (iv) pyramidal neurons in motor cortex (retrograde infection), and (v) brain terminals of spinothalamic neurons (anterograde infection).

population and can target a variety of spinal neurological disorders, including ALS, spinal trauma or chronic pain syndrome.

MATERIALS AND METHODS

Animals and general surgical preparation

These studies were carried out under protocols approved by the Institutional Animal Care and Use Committee of the Czech Academy of Sciences and by the Institutional Animal Care and Use Committees of the University of California, San Diego and were in compliance with The Association for Assessment of Laboratory Animal Care guidelines for animal use. All studies were performed in such a manner as to minimize group size and animal suffering.

Adult Sprague-Dawley rats (male and female, 250–350 g; *n* = 19; see Table 1 for experimental Groups) or adult minipigs resulting from cross-breeding of Minnesota and Gottingen strains (both sexes; 30–40 kg; *n* = 8; Table 1) were used. Rats were anesthetized with 5% isoflurane and maintained at 2–3% isoflurane during surgery depending on breathing rate and paw pinch response. The back of the rat was then shaved and cleaned with 2% chlorhexidine. After skin incision, the paravertebral muscle surrounding the cervical, thoracic or lumbar spinal vertebrae was removed, and animals were mounted into a spinal immobilization frame (Stoelting) using Cunningham's spinal clamps, as previously described.[12] To expose the spinal cord, a dorsal laminectomy of corresponding vertebra was performed using a dental drill. The dura was then cut open using a scalpel blade or 30G needle.

Minipigs were premedicated with intramuscular azaperonum (2 mg/kg) and atropine (1 mg/kg; Biotika, SK) and then induced with ketamine (20 mg/kg; i.v.). After induction, animals were intubated with a 2.5F tracheal tube. Anesthesia was maintained with 1.5% isoflurane in 50%/50% air/oxygen mixture at a constant 2 l/minute flow rate. Oxygen saturation was monitored throughout the procedure using a pulse oximeter (Nellcor Puritan Bennett, Ireland). After induction of anesthesia, animals were placed into a spinal immobilization apparatus, as described previously.[13] A dorsal laminectomy of Th5 or L2-L4 vertebrae, corresponding to Th5 or L3-L6 spinal segments, respectively, was then performed, and epidural fat removed using cotton swabs. The dura was cut open and secured to the surrounding tissue using 6.0 Proline (Figure 1c–e).

Placement of subpial catheter and subpial AAV9 injection

To place the subpial catheter, an L-shaped catheter guiding tube (18 or 23G) was constructed (Figure 1b). The guiding tube was mounted into an XYZ (Stoelting) manipulator and advanced to the surface of the exposed spinal segment. A 30G needle, previously bent at a 45° angle, was used to puncture the pia. The subpial catheter (PE-10 for pigs and PE-5 for rats) was then advanced into the subpial space from the guiding tube by manually pushing the catheter from the other end of the guiding tube. In rats, the catheter was advanced into the subpial space for about 1–1.5 cm and in pigs for about 3–6 cm. The virus was then injected into the SP space over 3 minutes using a 50 or 250 µl Hamilton syringe. After injection, the catheter was removed, dura closed using 6.0 Proline (in pigs only), and animals allowed to recover.

Placement of lumbar intrathecal catheter in rats

In some rats a lumbar intrathecal PE-5 catheter was placed. Under isoflurane anesthesia, an 8.5 cm PE-5 catheter (Spectranetics, Colorado Springs, CO) connected to 5 cm of polyethylene-PE-10 tube was inserted through an incision in the atlanto-occipital membrane of the cisterna magna.[14] The PE-10 catheter end was then externalized behind the head. Ten minutes after intrathecal AAV9 injection, the catheter was removed and the skin incision closed with 3.0 silk.

Preparation of AAV9 for *in vivo* injection

The 1.2 kb ubiquitin-C (UBC) promoter was made by oligonucleotide synthesis, linked with either eGFP or DsRed (RFP) and SV40 polyA signal, and cloned into a self-complementary double-strand DNA genome AAV (scAAV) vector plasmid.[15] Helper virus-free scAAV9 vectors expressing either eGFP or RFP driven by UBC promoter were produced by transient transfection of HEK293T cells with the vector plasmid pRep2-Cap9 and pAd-helper plasmids.[16] Plasmid pRep2-Cap9 was obtained from the Vector Core at the University of Pennsylvania. AAV vectors in the cell lysates prepared at 72 hours after transfection were purified as previously described and titered by Q-PCR.[15] The final titers were adjusted to 1.0×10^{13} genome copies per ml (gc/ml). Just before injection, the virus was mixed with dextran (10,000 MW) 1:1 to a final dextran concentration of 2.5%. The volume of subpial injectate was 30 µl in rats and 200 µl in pigs.

Perfusion fixation, postmortem *in situ* GFP fluorescence imaging, and immunofluorescence staining of spinal cord and brain sections

At 2–6 months after AAV9 delivery animals (rats and pigs; see Table 1) were deeply anesthetized with pentobarbital and transcardially perfused with 200 ml (rats) or 2,000 ml (pigs) of heparinized saline followed by 250 ml (rats) or 4,000 ml (pigs) of 4% paraformaldehyde in phosphate-buffered saline (PBS). The spinal cords and brains were dissected and post-fixed in 4% formaldehyde in PBS overnight at 4 °C. After postfixation, the whole spinal cord(s) was imaged *in situ* using Spectrum optical imaging system (Xenogen, Alameda, CA). Sequences were acquired at excitation wavelength 465 nm and emission wavelength 520 nm. Medium binning was used, and the exposure time was 3 seconds. Images were analyzed using Living Image 4.3.1 (Xenogen, Alameda, CA) software. The signals were calculated using fixed volume region of interests (ROIs). Spinal cords were then cryoprotected in 30% sucrose PBS until transverse or longitudinal sections (30-µm-thick) were cut on a cryostat and stored in PBS.

Prepared sections were immunostained overnight at 4°C with the following primary antibodies made in PBS with 0.2% Triton X-100: rabbit anti-GFAP (1:500, Origene, Rockville, MD), mouse anti-neuronal nuclei antigen (NeuN, 1:1,000, Chemicon, Temecula, CA), mouse anti-oligodendrocyte (adenomatosis polyposis coli (APC) (CC1); 1:500; Millipore), mouse anti-endothelial (RECA-1; 1: 1,000; Abcam, Cambridge, MA). No anti-GFP or anti-RFP antibody was used.

After incubation with primary antibodies, sections were washed three times in PBS and incubated with fluorescent-conjugated secondary

---

Table 1 Experimental groups

Animal model	Adult SD rat			Adult minipig		
Segmental level	Cervical	Thoracic	Lumbar	Cervical	Thoracic	Lumbar
Intrathecal AAV9	–	–	N=5 (&)	–	–	–
Subpial AAV9	N=4*; N=4*(&)	–	N=6 (#)	–	N=4 (&)	N=4 (#)

*-AAV9-UBI-GFP; *-AAV9-UBI-RFP; (#)-6 months survival; (&) – 6–8 weeks months survival.

Table 2 Quantification (%) of GFP expressing NeuN+ interneurons and α-motoneurons at 6 months after lumbar (L2) subpial AAV9-UBI delivery in SD rat and minipig

Segment(s)	Neuron type	Th10	Th11	Th12	L1	L2	L3	L4	L5	L6	S1
SD rat (n = 3)	α-moto	78 ± 9	87 ± 11	90 ± 6	89 ± 6	95 ± 4	94 ± 6	93 ± 5	88 ± 6	99 ± 3	91 ± 8
	Intern.	96 ± 4	93 ± 5	96 ± 7	98 ± 6	97 ± 2	92 ± 3	81 ± 9	72 ± 9	77 ± 11	90 ± 6
Minipig (n = 3)	α-moto	56 ± 14	54 ± 8	76 ± 12	94 ± 2	92 ± 6	94 ± 7	78 ± 9	56 ± 14	49 ± 16	50 ± 11
	Intern.	90 ± 11	90 ± 7	89 ± 4	96 ± 4	98 ± 2	90 ± 7	83 ± 11	76 ± 16	80 ± 12	82 ± 16

α-moto-α-motoneurons; Intern.- interneurons.

npg

Potent spinal parenchymal AAV9-mediated gene delivery by subpial injection in adult rats and pigs
A Miyanohara et al.

10

donkey anti-rabbit and donkey anti-mouse antibodies (Alexa Fluor 488, 546 or 647, 1:1,000, Invitrogen, Waltham, MA), respectively, and DAPI for general nuclear staining. In sections expressing AAV9-UBI-induced GFP, Alexa Fluor 594 or 647 was used, while Alexa 488 or 647 was employed as secondary antibody in sections expressing AAV9-UBI-induced RFP.

Sections were then mounted on slides, dried at room temperature and covered with a Prolong anti-fade kit (Invitrogen). Fluorescence images were captured using a Zeiss Imager M2 microscope and confocal images were taken using an Olympus FV1000 microscope.

Quantitative analysis and densitometry measurement of neuronal AAV9-UBI-induced GFP expression

To determine the threshold of AAV9-induced GFP expression, densitometry analysis of GFP signal was performed and compared to naive controls. Images were captured from serially cut transverse sections taken from above, at the center and below the level of subpial AAV9 injection as well as from naive-noninjected animals. All sections were stained with NeuN antibody. Because of the very high intensity of AAV9-induced GFP signal, *no* anti-GFP staining was used. Mosaic images (tile scan) captured from selected sections using identical lamp and exposure time intensity (the lamp is set to 50% and the exposure time is 5 ms) were then collected. The intensity of GFP signal in neuronal bodies was then compared to naive controls and the threshold that identified GFP positive neurons determined using signal densitometry (Supplementary Figure S2). Percentage of GFP positive NeuN+ neurons (interneurons, α-motoneurons) was then estimated and quantified in individual segments respective to the segment of subpial AAV9 delivery. For quantification, rats ($n = 3$) and pigs ($n = 3$) previously injected with L2 subpial AAV9-UBI-GFP and surviving for 6 months were used (Table 2). Three sections taken from each segment of each animal were used for quantification.

Analysis of motor and sensory function

The long-term (6 months' survival) effect of lumbar subpial AAV9-UBI-GFP delivery on neurological function was analyzed in six rats and four pigs in 7-day intervals.

Open-field locomotion testing in rats. Changes in motor function in the rat was assessed using a Basso, Beattie, Bresnahan open-field 21 grade locomotion rating scale.[17]

Analysis of motor function in pigs. The previously developed 14 grade porcine motor scoring system was used.[18] In both models, the presence of allodynia was tested by presence/absence of vocalization/withdrawal from touching the trunk below the level of subpial AAV9 delivery with a 20 g von Frey filament (rats) or by skin pinch (pigs).

REFERENCES

1. Foust, KD, Nurre, E, Montgomery, CL, Hernandez, A, Chan, CM and Kaspar, BK (2009). Intravascular AAV9 preferentially targets neonatal neurons and adult astrocytes. *Nat Biotechnol* **27**: 59–65.
2. Duque, S, Joussemet, B, Riviere, C, Marais, T, Dubreil, L, Douar, AM et al. (2009). Intravenous administration of self-complementary AAV9 enables transgene delivery to adult motor neurons. *Mol Ther* **17**: 1187–1196.
3. Gray, SJ, Matagne, V, Bachaboina, L, Yadav, S, Ojeda, SR and Samulski, RJ (2011). Preclinical differences of intravascular AAV9 delivery to neurons and glia: a comparative study of adult mice and nonhuman primates. *Mol Ther* **19**: 1058–1069.
4. Meyer, K, Ferraiuolo, L, Schmelzer, L, Braun, L, McGovern, V, Likhite, S et al. (2015). Improving single injection CSF delivery of AAV9-mediated gene therapy for SMA: a dose-response study in mice and nonhuman primates. *Mol Ther* **23**: 477–487.
5. Foust, KD, Salazar, DL, Likhite, S, Ferraiuolo, L, Ditsworth, D, Ilieva, H et al. (2013). Therapeutic AAV9-mediated suppression of mutant SOD1 slows disease progression and extends survival in models of inherited ALS. *Mol Ther* **21**: 2148–2159.
6. Passini, MA, Bu, J, Richards, AM, Treleaven, CM, Sullivan, JA, O'Riordan, CR et al. (2014). Translational fidelity of intrathecal delivery of self-complementary AAV9-survival motor neuron 1 for spinal muscular atrophy. *Hum Gene Ther* **25**: 619–630.
7. Bell, P, Hinderer, C, Louboutin, JP, Yu, H, Grant, R, Bote, E et al. (2015). Motor neuron transduction after intracisternal delivery of AAV9 in a cynomolgus macaque. *Hum Gene Ther Methods* **26**: 43–44.
8. Nihei, K, McKee, AC and Kowall, NW (1993). Patterns of neuronal degeneration in the motor cortex of amyotrophic lateral sclerosis patients. *Acta Neuropathol* **86**: 55–64.
9. Conradi, S and Ronnevi, LO (1993). Selective vulnerability of alpha motor neurons in ALS: relation to autoantibodies toward acetylcholinesterase (AChE) in ALS patients. *Brain Res Bull* **30**: 369–371.
10. Hefferan, MP, Galik, J, Kakinohana, O, Sekerkova, G, Santucci, C, Marsala, S et al. (2012). Human neural stem cell replacement therapy for amyotrophic lateral sclerosis by spinal transplantation. *PLoS One* **7**: e42614.
11. Samaranch, L, San Sebastian, W, Kells, AP, Salegio, EA, Heller, G, Bringas, JR et al. (2014). AAV9-mediated expression of a non-self protein in nonhuman primate central nervous system triggers widespread neuroinflammation driven by antigen-presenting cell transduction. *Mol Ther* **22**: 329–337.
12. Kakinohana, O, Cizkova, D, Tomori, Z, Hedlund, E, Marsala, S, Isacson, O et al. (2004). Region-specific cell grafting into cervical and lumbar spinal cord in rat: a qualitative and quantitative stereological study. *Exp Neurol* **190**: 122–132.
13. Usvald, D, Vodicka, P, Hlucilova, J, Prochazka, R, Motlik, J, Kuchorova, K et al. (2010). Analysis of dosing regimen and reproducibility of intraspinal grafting of human spinal stem cells in immunosuppressed minipigs. *Cell Transplant* **19**: 1103–1122.
14. Yaksh, TL and Rudy, TA (1976). Analgesia mediated by a direct spinal action of narcotics. *Science* **192**: 1357–1358.
15. Xu, Q, Chou, B, Fitzsimmons, B, Miyanohara, A, Shubayev, V, Santucci, C et al. (2012). *In vivo* gene knockdown in rat dorsal root ganglia mediated by self-complementary adeno-associated virus serotype 5 following intrathecal delivery. *PLoS One* **7**: e32581.
16. Xiao, X, Li, J and Samulski, RJ (1998). Production of high-titer recombinant adeno-associated virus vectors in the absence of helper adenovirus. *J Virol* **72**: 2224–2232.
17. Basso, DM, Beattie, MS and Bresnahan, JC (1995). A sensitive and reliable locomotor rating scale for open field testing in rats. *J Neurotrauma* **12**: 1–21.
18. Navarro, R, Juhas, S, Keshavarzi, S, Juhasova, J, Motlik, J, Johe, K et al. (2012). Chronic spinal compression model in minipigs: a systematic behavioral, qualitative, and quantitative neuropathological study. *J Neurotrauma* **29**: 499–513.

Supplementary Information accompanies this paper on the *Molecular Therapy—Methods & Clinical Development* website (http://www.nature.com/mtm)